Simulation of a-Si PV System Linked to the Grid by DC-DC Boost and Two-level Converter

L. Fialho, R. Melício, V.M.F. Mendes
Department of Physics, Universidade de Évora,
Évora, Portugal
IDMEC/LAETA, Instituto Superior Técnico, Universidade
de Lisboa, Lisbon, Portugal
ruimelicio@uevora.pt

L. Rodrigues, S. Viana, A. Estanqueiro
Laboratório Nacional de Energia e Geologia,
Lisbon, Portugal

Abstract—**This paper is about a PV system linked to the electric grid by power electronic converters. The modeling for the converters emulates the association of a DC-DC boost with a two-level power inverter in order to follow the performance of a testing commercial inverter employed on an experimental system. It is used pulse width modulation by sliding mode control associated with space vector modulation for control the boost and the inverter. The PV system is described by the five parameters equivalent circuit and parameter identification is carried out. Maximum power point tracking is implemented by a $\partial P/\partial V$ procedure. Simulation studies are performed and a comparison with the testing experimental system is presented.**

Keywords-photovoltaic energy; MPPT; modeling; power electronics; simulation; experimental results.

I. INTRODUCTION

Electricity market restructuring offers more flexibility at both levels of generation and consumption [1]. Also, with the restructuring in the power system sector, the developments in distributed power generation systems (PGSs) opened new opportunities for the electric sector [2]. Distributed PGSs include, for instance, photovoltaic, wind power, wave, small hydropower, geothermal and fuel cells. A summary of the hardware configuration for some distributed PGSs is given in [3] and a review of control and grid integration for distributed PGSs is given in [4].

The development of photovoltaic power generation is significant in recent years, is foreseen as able to compete with the traditional fossil-fuelled thermal power generation, particularly, taken into consideration the environmental safeguarding value [5,6]. Climate changes and the environmental policy are becoming progressively important for electric companies as pollution regulations become more strict, and customer perception of environmental effects is increasing. Nowadays it is known that the greenhouse effect can be decelerated only if CO_2 anthropogenic emissions are reduced [7]. The European Commission committed Europe to become a highly energy-efficient, low-carbon economy, and were enacted through the climate and energy package that a set of proposals to create a new Energy Policy for Europe,

reducing its own anthropogenic emissions by 20% by 2020 and 50% until 2050, raising the share of EU energy consumption produced from renewable resources. In the future it is expected that solar energy will be a significant part of the European Energy Policy. European Commission considers that smart grids marks a new advance towards a more active consumer role, improved integration of renewable energy sources into the grid, increased energy efficiency and a significant impact on reducing the anthropogenic emissions, job creation and technological development in the Union. In Portugal, the renewable energy reached a total installed capacity of 10887 MW in March 2014. The photovoltaic generation capacity is 297 MW and continues increasing.

A photovoltaic system converts solar energy into electric energy using a solar cell. Cells may be assembled to form panels and arrays. A PV array can be a panel or a set of panels connected in series or parallel to form large PV systems without or with tracking systems in order to meet higher values of energy conversion during sunny days due to the diverse perpendicular positions to collect the sun´s irradiation [8,9].

Modern power electronic converters have been developed for integration of renewable energy sources in the electric grid [9,10]. The power electronic converters, e.g. inverters, allow operating the PV system and improve the power extraction. The inverter is in employment by two reasons. First, serves as a link between the low DC voltage at the output of the PV system and the AC voltage of the electric grid. Second, allows tracking the Maximum Power Point (MPP), i.e., the processing has to incorporate this functionality to avoid the fact that the power delivered from the modules is sensitive to the point of operation [11]. For instance, a tracking process based on $\partial P/\partial V$ feedback is in use on PV systems to adjust the converters IGBT's to achieve the MPP energy conversion [9].

In this paper, it is considered a silicon amorphous PV system implemented with a DC-DC boost and a two-level inverter (TLI) topologies. The paper is organized as follows. Section II presents the model for the PV system, DC-DC boost and TLI topologies. Section III presents the control strategy,

consisting in pulse width modulation (PWM) by space vector modulation (SVM) associated with sliding mode (SM) for controlling the converter. Section IV presents a case study: an assessment by simulation and comparison with experimental results of an amorphous technology PV system linked to the electric grid by a commercial inverter. Finally, conclusions are given in Section V.

II. MODELING

A. PV Module

The solar cells are considered to be subjected to the same G solar irradiance and T p-n junction temperature. Hence, the equivalent circuit of a cell is also the one for the PV system. The equivalent circuit chosen for the PV system simulation consists in a current controlled generator, a single-diode, a shunt and series resistances. This equivalent circuit is shown in Fig. 1.
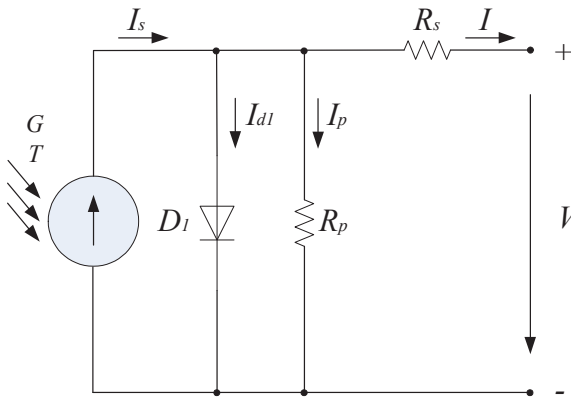

Figure 1. Equivalent circuit for a PV module.

R_p and R_S are respectively the equivalent shunt and the series resistances, I_L is the photo generated electric current, I_{d1} is the current at diode D_1, I_p is the leakage current, I is the output current at the terminals of module, V is the output voltage at the terminals of module. The I-V characteristic associated with the equivalent circuit of five parameters [8,12] obeys the relation given by given by

$$I = I_s - I_0(e^{\frac{V+IR_s}{mV_T}} - 1) - \frac{V+IR_s}{R_p}. \quad (1)$$

(1) is an implicit function where I_0 is the diode reverse bias saturation current, m is the ideality factor, V_T is the p-n junction thermal voltage. Hence, (1) has to be solved using, for instance, the iterative method of Newton-Raphson.

The incremental conductance (INC) at MPP [8,12] is given by

$$\left(\frac{\partial I}{\partial V}\right)_{MP} = -\frac{V_{MP} - I_{MP}R_s}{V_{MP}}\left(\frac{I_0 e^{\frac{V_{MP}+I_{MP}R_s}{mV_T}}}{mV_T} + \frac{1}{R_p}\right). \quad (2)$$

The resistance R_p [8,12] is approximated by the expression given by

$$R_p \approx \frac{(V_{MP} - I_{MP}R_s)V_{MP} - mV_T V_{MP}}{(V_{MP} - I_{MP}R_s)(I_{sc} - I_{MP}) - mV_T I_{MP}} - R_s. \quad (3)$$

The ideality factor at MPP [8,12] is given by

$$m \approx \frac{V_{oc} - V_{MP} - I_{MP}R_s}{V_T \ln\left[\frac{I_{sc}(R_s + R_p) - V_{oc}}{(I_{sc} - I_{MP})(R_s + R_p) - V_{MP}}\right]}. \quad (4)$$

B. MPPT Algorithm

The input parameters are values of the voltage and current of the PV system. The criterion is to follow the condition given by $\partial P/\partial V = 0$, i.e., if the condition is met, then the algorithm has found the MPP point. But typically the algorithm iterates around that condition until eventually converges. The iterations procedures are as follow: if $\partial P/\partial V > 0$, an incremental adjustment is set in order to increase the out voltage, i.e., in the direction of the MPP; if $\partial P/\partial V < 0$, an adjustment is set in order to decrease the out voltage to be in the right tracking for the MPP [9].

C. DC-DC Boost Converter

The DC-DC boost converter has one unidirectional commanded IGBT, i.e., transistor S_0. The DC-DC boost converter is connected between the PV modules and a capacity bank, which in turn is connected to a TLI.

For the switching function of the DC-DC boost converter, the switching variable λ is used to identify the state of the IGBT S_0 of the boost converter and the switching variable $\bar{\lambda}$ is used to identify the state of the diode D_0 of the boost. The two conditions [13] for the switching variable of the DC-DC boost are given by

$$\begin{cases} \lambda = 1 \text{ and } \bar{\lambda} = 0 \ (S_0 = 1 \text{ and } D_0 = 0) \\ \lambda = 0 \text{ and } \bar{\lambda} = 1 \ (S_0 = 0 \text{ and } D_0 = 1) \end{cases}. \quad (5)$$

The module current I is modeled by the state equation given by

$$\frac{dI}{dt} = \frac{1}{L_s}[V - \bar{\lambda}(V_{D0} + V_{dc})]. \quad (6)$$

where V_{D0} is the diode forward voltage at direct current, V_{dc} is the capacitor voltage. The capacitor voltage V_{dc} is modeled by the state equation given by by

$$\frac{dv_{dc}}{dt} = \frac{1}{C}(\overline{\lambda}\, I - i_I)\ . \tag{7}$$

where i_I is the current injected on the inverter.

D. TLI

The TLI is connected between a capacity bank and a second order filter, which in turn is connected to the electric grid, modeled by a three-phase active symmetrical circuit. The TLI is a DC-AC converter, with six unidirectional commanded transistors S_{iy} used as an inverter. The groups of two transistors linked to the same phase constitute a leg y of the converter. The TLI modeling [14] assumes that: 1) the diodes are ideal: in conduction is null the voltage between the terminals, and in blockade is null the current at the terminals; 2) the transistors are ideal and unidirectional, and they will never be subject to inverse voltages, being this situation guaranteed by the anti-parallel diodes; 3) the voltage in the exit of the boost converter should always be $v_{dc} > 0$; 4) each leg y of the converter should always have one transistor on a conduction state. The switching function of each transistor is used the switching variable γ_y to identify the state of the transistor i in the leg y of the converter. The index h with $h \in \{a,b\}$ identifies the IGBT. The index y with $y \in \{a,b,c\}$ identifies a leg of the inverter. The two conditions [14] for the γ_y of each leg y are given by

$$\gamma_y = \begin{cases} 1, & (S_{ay} = 1 \text{ and } S_{by} = 0) \\ 0, & (S_{ay} = 0 \text{ and } S_{by} = 1) \end{cases} \quad y \in \{a, b, c\}. \tag{8}$$

The restriction for the leg y [14] is given by

$$\sum_{i=1}^{2} S_{iy} = 1 \quad y \in \{a, b, c\}. \tag{9}$$

E. PV system configuration

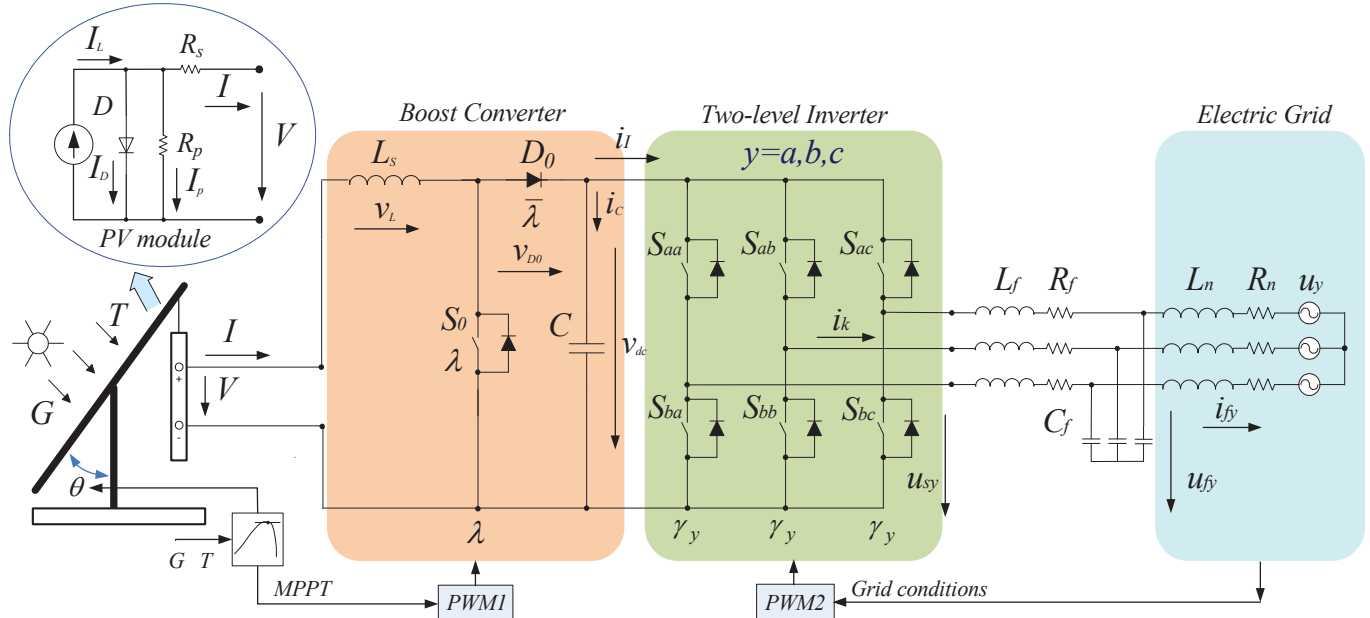The configuration for the PV system is shown in Fig. 2.

Figure 2.   PV system model with DC-DC boost and TLI.

III.   CONTROL STRATEGY

Power converters are variable structures, because of the on/off switching states of the transistors. PI controllers in order to obtain current references and PWM by SVM associated with SM is used for convenient controlling of the power converters. The SM control strategy is an option known by the advantage of having attractive features such as considerable robustness to parametric uncertainties due to the partial shading and the electric grid disturbances [13,14]. The MPPT method to assess the MPP operates by making convenient adjustments over the DC-DC boost converter in order to follow the condition given by $\partial P/\partial V = 0$.

The output vectors for level 0 and level 1 in the $\alpha\beta$ plane for the TLI [13,14] are shown in Fig. 3.

SM control is particularly interesting in systems with variable structure, such as switching power inverter, ensuring the choice of the appropriate space vectors. Their aim is to let the system slide along a predefined sliding surface $A(e_{\alpha\beta}, t)$ by changing the system structure.
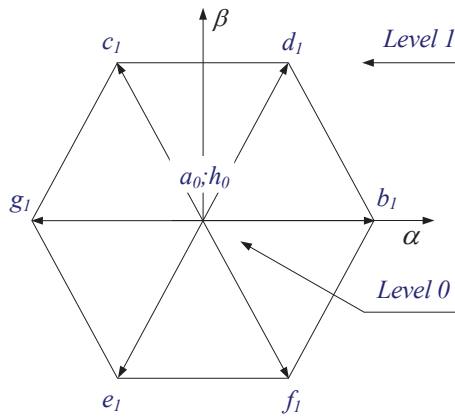
Figure 3.   TLI, output space vectors.

The transistors present physical limitations, since they cannot switch at infinite frequency. Also, for a finite value of the switching frequency, an error will exist between the control value and the reference value $e_{\alpha\beta}$.

The vector selection in order to ensure stability for the TLI [14] is shown in Table I.

TABLE I.   OUTPUT VECTORS SELECTION FOR THE TLI

$\delta_\beta \setminus \delta_\alpha$	-1	0	1
-1	e_1	$e_1;f_1$	f_1
0	g_1	$a_0;h_0$	b_1
1	c_1	$c_1;d_1$	d_1

The system slide along the $A(e_{\alpha\beta},t)$ is guaranteed if the state trajectory near the surfaces satisfied the following condition [14] given by

$$A(e_{\alpha\beta},t) \frac{dA(e_{\alpha\beta},t)}{dt} < 0 . \qquad (10)$$

IV.   CASE STUDY

The model for the configuration shown in Fig. 2, the MPPT algorithm, the control strategy is implemented in Matlab/Simulink.

The simulation is carried out for a silicon amorphous PV module situated in LNEG, with the coordinates 38°46'18.50' N, 9°10'38.50' W. The data for the silicon amorphous solar module Kaneka KA 58 at STC [15] is shown in Table II. The simulation results are compared with experimental observation carried out for the amorphous PV technology.

The simulated, green, and experimental, blue, curves for I-V; the absolute error, red, and MPP at STC conditions are shown in Fig. 4.
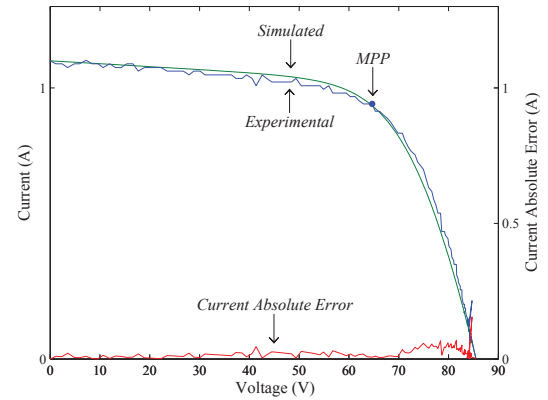

Figure 4.   I-V curves simulated and experimental.

The simulated, green, and experimental, blue, curves for P-V; the absolute error, red, and MPP at STC conditions are shown in Fig. 5.
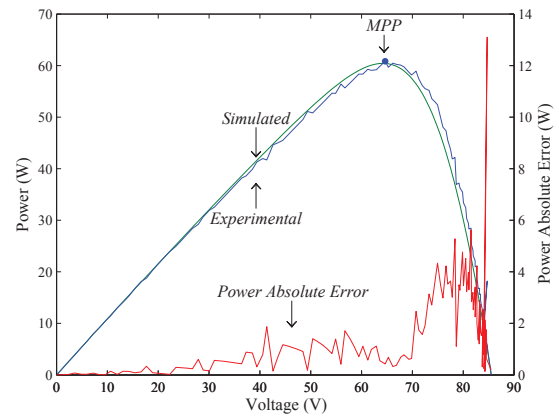

Figure 5.   P-V curves simulated and experimental.

The current injected into the grid, simulated, green, experimental, blue, and the absolute error on the current are shown in Fig. 6.
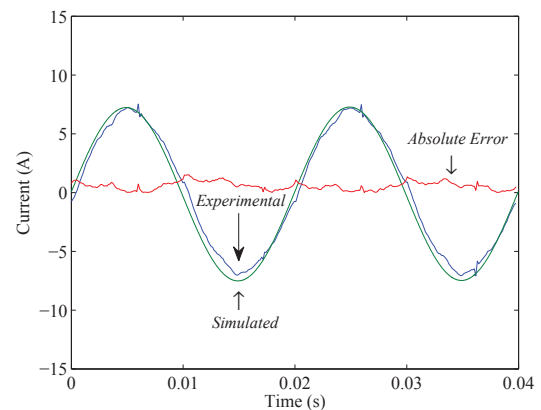

Figure 6.   Electric grid current injected.

TABLE II. DATA FOR KANEKA KA58 SOLAR MODULE AT STC

Technology	V_{MP}^*	I_{MP}^*	V_{oc}^*	I_{sc}^*
Amorphous	63 V	0.92 A	85 V	1.12 A

The simulations root mean square error (RMSE) for the I-V characteristic curve, P-V curve and current injected into the grid is shown in Table III.

TABLE III. SIMULATIONS ROOT MEAN SQUARE ERROR (RMSE)

Simulation	I-V Curve	P-V Curve	Current injected into the electric grid
RMSE	0.0293 A	2.2328 W	0.6656 A

Both RMSE are a small relative value of the respective rated values, showing that the modeling is appropriated for describing the PV system linked to the grid by the commercial inverter in this case study. The THD of the simulated current injected into the electric grid is 0.24% and the THD of the experimental current injected in the electric grid is 0.88% during normal operation of the PV system. The percentage of the fundamental component calculated by the DFT for the simulated current injected into the grid is 91.2% and for the experimental current injected into the grid is 79.5%. Those differences between the respective percentages are believed to happen impart due to the fact that the electric grid is not a perfect ideal source of voltage.

The PV system with DC-DC boost and two-level power inverter topology has an adequate performance in what regards the fact that the THD of the output current is lower than 5% limit imposed by IEEE-519 standard. The dominant harmonic of the current injected into the electric grid computed by the DFT for the simulated and the experimental PV systems is the 3rd harmonic with 0.7%. A comparison between simulated and the experimental results shows a satisfactory accomplishment in this modeling for the PV system at experimental testing.

The switching frequency for IGBTs is 6 kHz.

V. CONCLUSIONS

Simulation studies on PV systems are essential to assists the engineers in what regards extracting the maximum energy, anticipating performance and deciding convenient measures to avoid malfunctions.

A modeling for a PV system with DC-DC boost and two-level power inverter topology is proposed using the equivalent five parameter for PV modules; and DC-DC boost and two-level power inverter topology modeling, assuming a control strategy by PI controllers and pulse width modulation by space vector modulation associated with sliding mode.

The application of this modeling to a case study on a silicon amorphous solar module Kaneka KA 58 with a commercial inverter with a convenient filtering allows to anticipate a THD for the output current lower than the 5% limit imposed by IEEE-519 standard for the PV system with DC-DC boost and two-level power inverter topology.

Although disregarding the fact that the electric grid is not a perfect source of energy, the experimental results show a tolerable concordance with the simulated ones.

REFERENCES

[1] A. Poullikas, "A comparative assessment of net metering and feed in tariff schemes for residential PV systems," Sust. Energy Technologies and Assessments, vol. 3, pp. 1-8, September 2013

[2] J. Peças Lopes, N. Hatziargyriou, J. Mutale, P. Djapic, and N. Jenkins, "Integrating distributed generation into electric power systems: a review of drivers, challenges and opportunities," Electric Power Systems Research, vol. 77, pp. 1189-1203, July 2007.

[3] F. Blaabjerg, Z. Chen, and S.B. Kjaer, "Power electronics as efficient interface in dispersed power generation systems," IEEE Transactions Industrial Electronics, vol. 19, pp. 1184-1194, September 2004.

[4] F. Blaabjerg, R. Teodoresco, M. Liserre, and A.V. Timbus, "Overview of control and grid synchronization for distributed power generation systems," IEEE Transactions Industrial Electronics, vol. 53, pp. 1398-1409, October 2006.

[5] M.C. Di Piazza, M. Pucci, and G. Vitale, "Intelligent power conversion system management for photovoltaic generation," Sust. Energy Tech. and Assessments, vol. 2, pp. 1-30, June 2013.

[6] H.A. Kazem, and T. Khatib, "Techno-economical assessment of grid connected photovoltaic power systems productivity in Sohar, Oman," Sust. Energy Technologies and Assessments, vol. 3, pp. 61-65, September 2013.

[7] D. Smith, P.J. Mago, and N. Fumo, "Benefits of thermal energy storage option combined with CHP system for different commercial building types," Sust. Energy Technologies and Assessments, vol. 1, pp. 3-12, March 2013.

[8] L. Fialho, R. Melício, V. M. F. Mendes, J. Figueiredo, and M. Collares-Pereira, "Effect of shading on series solar modules: simulation and experimental results," in Proc. Conf. Electronics, Telecomunications and Computers, pp. 1-8, 2013.

[9] R.J. Pereira, R. Melício, V. M. F. Mendes, and A. Joyce, "PV system with maximum power point tracking: modeling, simulation and experimental results," in Proc. Conf. Electronics, Telecomunications and Computers, pp. 1-7, 2013.

[10] E. Koutroulis, and F. Blaabjerg, "Methods for the optimal design of grid-connected PV inverters," International Journal Renewable Energy Research, vol. 1, pp. 54-64, 2011.

[11] Y. Yang, and F.P. Zhao, "Adaptive perturb and observe MPPT technique for grid-connected photovoltaic inverters," Procedia Engineering, vol. 23, pp. 468-473, 2011.

[12] C. Carrero, J. Rodríguez, D. Ramírez and C. Platero, "Accurate and fast convergence method for parameter estimation of PV generators based on three main points of the I–V curve," Renewable Energy, vol. 36, pp. 2972-2977, November 2011.

[13] J.F. Silva, "Control methods for power converters," in Handbook of Power Electronics, Ed. M. H. Rashid, New York, 2001, pp. 6-10.

[14] R. Melício, and V.M.F. Mendes, "Simulation of Power Converters for Wind Energy Systems," Información Tecnológica, vol. 18, pp. 25-34, July-August 2007.

[15] Kaneka Photovoltaic Products Inform. http://www.pv.kaneka.co.jp